

MILOS SEDLACEK, MICHAL KRUMPHOLC

Czech Technical University in Prague
Faculty of Electrical Engineering
CZ-166 27 Czech Republic, e-mail sedlaceM@fel.cvut.cz

DIGITAL MEASUREMENT OF PHASE DIFFERENCE - A COMPARATIVE STUDY OF DSP ALGORITHMS

The paper compares nine methods of measurement of the phase difference of digitized sinusoidal signals mainly according to their sensitivity to sampling non-integer number of signal periods. The investigated methods can be classified into four groups - modifications of classical zero-crossing based measurements, virtual vector voltmeter, DFT-based measurements, and modifications of sine-wave fit algorithm. Results of both simulations and measurements are presented.

Keywords: phase difference measurement, DSP algorithms of phase difference estimation

1. INTRODUCTION

This paper is enlarged and updated version of [1]. Measurement of phase difference of two harmonic signals is used e.g. by measurement of phase frequency characteristics of linear circuits or measurement of impedances. The classical approach is based on detection of zero crossings of signals [2, 3]. Other methods are based on virtual vector voltmeter, on DFT (e.g. [4]) and on sine-wave-fit algorithms (e.g. [5]). Altogether 9 methods based on the above mentioned principles were investigated. The methods are compared primarily from the points of view of their sensitivity to sampling non-integer number of signal periods ("non-coherent sampling"). The paper is in a sense a continuation of [6] where comparison was based on coherent sampling only and windowed and interpolated DFT [7, 8] and a recently published modification of sine-wave-fit [11] were not included. MATLAB environment was used for both simulations and measurements.

2. THE INVESTIGATED METHODS

2.1. Methods based on zero-crossings detection (ZCRF and ZCRR)

These methods are based on the classical phase difference estimation algorithm. Detections of crossing a zero level by both the measured signals is used for phase difference estimation e.g. using universal counters or dual-channel oscilloscopes. Its principle is shown in Fig. 1 and in relation (1). Local linear interpolation around zero crossings (between two signal samples with different signs) allows resolution increase. Signal pre-processing before detection of crossings of zero level is often required in practice to prevent additional zero-crossings caused by additive noise and/or signal higher harmonic components.

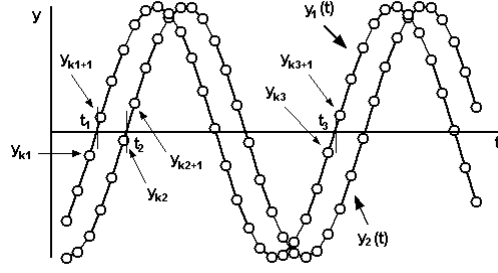


Fig. 1. Principle of phase difference estimation by zero crossings detection.

We have investigated two types of this signal pre-processing – LP filtering (using IIR or FIR digital filters) and moving averaging (method denoted here “ZCRF” - stands for “Zero CRossing with Filtration”) or moving average and linear regression in surroundings of zero crossings (method “ZCRR”, abbreviation of “Zero-Crossing with Regression”).

$$\varphi = 2\pi \frac{t_2 - t_1}{t_3 - t_1} \quad (\text{rad}). \quad (1)$$

2.2. Method based on virtual vector-voltmeter (VVV)

This method uses multiplication of the signal by a reference signal (sinusoid of the same frequency as frequency of the measured signals) and finding mean value (DC component) of this product. This mean value is proportional to cosine of the phase difference between the fundamental harmonic component of the measured signal and the reference signal, the phase shift of which is considered to be zero. This mean gives also the real part of the phasor (vector) of the measured signal. Multiplying the signal by cosine reference signal (i.e. reference signal shifted by 90° with reference to the first one) and finding the mean (e.g. by low-pass filter) gives the imaginary part of the phasor U_1 of measured signal. Phase difference of the measured signal and the reference signal can be found afterwards by means of $\arctg(\text{Im}U_1/\text{Re}U_1)$ function. Using the same procedure for the second measured signal allows finding the phase difference between the second signal and the reference signal. Difference of phase shifts of the two signals referred to reference signal is the measured phase difference (phase difference of their fundamental harmonic components in case of sinusoidal signals distorted by higher harmonic components). The both signals' amplitudes are found together with phase difference. The just described procedure can be expressed by the equations below. The two measured signals (continuous in time) can be written as

$$v_1(t) = V_1 \sin(\omega_{\text{sig}} t + \varphi_1), \quad (2)$$

$$v_2(t) = V_2 \sin(\omega_{\text{sig}} t + \varphi_2), \quad (3)$$

where V_1 , φ_1 , and V_2 , φ_2 are the unknown magnitudes and phases of the first and the second signal, and the $\omega_{\text{sig}} = 2\pi f_{\text{sig}}$ is a signal circular frequency.

Time-discrete version of these signals are

$$v_1(nT) = V_1 \sin(\omega_{\text{sig}} nT + \varphi_1), \quad (4)$$

$$v_2(nT) = V_2 \sin(\omega_{\text{sig}} nT + \varphi_2), \quad (5)$$

where T is sampling interval ($T=1/f_s$, f_s being sampling frequency).

The two (discrete-time) *reference signals* have the same frequency as the measured signals and can be expressed as

$$v_{R1}(nT) = V_R \sin(\omega_{sig} nT), \quad (6)$$

$$v_{R2}(nT) = V_R \cos(\omega_{sig} nT). \quad (7)$$

The four mean values of the products of input signals $v_1(t)$ and $v_2(t)$ with the reference signals $v_{R1}(t)$ and $v_{R2}(t)$ are

$$V_{11} = \frac{1}{N} \sum_{n=0}^{N-1} v_1(nT)v_{R1}(nT), \quad (8)$$

$$V_{12} = \frac{1}{N} \sum_{n=0}^{N-1} v_1(nT)v_{R2}(nT), \quad (9)$$

$$V_{21} = \frac{1}{N} \sum_{n=0}^{N-1} v_2(nT)v_{R1}(nT), \quad (10)$$

$$V_{22} = \frac{1}{N} \sum_{n=0}^{N-1} v_2(nT)v_{R2}(nT), \quad (11)$$

where N is the total number of sampled values of each signal. These values are proportional to the real (V_{12} and V_{22}) and to the imaginary (V_{11} and V_{21}) parts of the sinusoidal input signal voltage phasors (vectors) \mathbf{V}_1 and \mathbf{V}_2 . The phases of the two input signal voltages can be found as

$$\varphi_1 = \arctg \frac{\text{Im}(\mathbf{V}_1)}{\text{Re}(\mathbf{V}_1)} = \arctg \frac{\frac{1}{N} \sum_{n=0}^{N-1} v_1(nT)v_{R1}(nT)}{\frac{1}{N} \sum_{n=0}^{N-1} v_1(nT)v_{R2}(nT)} = \arctg \frac{\sum_{n=0}^{N-1} v_1(nT)v_{R1}(nT)}{\sum_{n=0}^{N-1} v_1(nT)v_{R2}(nT)}, \quad (12)$$

$$\varphi_2 = \arctg \frac{\text{Im}(\mathbf{V}_2)}{\text{Re}(\mathbf{V}_2)} = \arctg \frac{\frac{c}{N} \sum_{n=0}^{N-1} v_2(nT)v_{R1}(nT)}{\frac{c}{N} \sum_{n=0}^{N-1} v_2(nT)v_{R2}(nT)} = \arctg \frac{\sum_{n=0}^{N-1} v_2(nT)v_{R1}(nT)}{\sum_{n=0}^{N-1} v_2(nT)v_{R2}(nT)}. \quad (13)$$

The phase difference to be found is

$$\varphi = \varphi_2 - \varphi_1. \quad (14)$$

The phases of the two phasors are from (12) and (13) found correctly, if integer number of signal periods is sampled. Bias of measurement of phase difference occurs in (14), if condition of coherent sampling $NT = m T_{sig}$ (m being positive integer number) is not fulfilled. In that case the mean values in (8) to (11) are not calculated from integer number of signal periods and differ from the mean value across one period.

2.3. Methods based on DFT (DFT, IDFT)

The well-known Discrete Fourier Transform algorithm is computed for N signal samples (N is DFT length). The DFT spectrum is periodical spectrum with period N and it is discrete in frequency.

If the measured signal is finite in time (e.g. a selected part of time-discrete signal of the length NT , as in our case), the DFT spectrum $X(k)$ can be found by sampling the spectrum found by definition from infinitely long sequence of signal samples by the so-called Fourier Transform of Discrete Signals - FTD (called also Discrete-Time Fourier Transform - DTFT) $X(e^{j\omega T})$ [14]. This spectrum is continuous function of circular frequency ω periodic with period equal to sampling circular frequency ω_s , and the argument in the FTD spectrum $X(e^{j\omega T})$ stresses this periodicity. DFT spectrum is (contrary to FTD spectrum) discrete in frequency and consists of samples of the FTD spectrum in values of circular frequencies $\omega_k = k \times (\omega_s/N)$, ω_s being sampling circular frequency.

The phase difference between fundamental harmonic components of the two measured signals is found as the phase difference of the fundamental harmonics DFT phase spectrum values (method "DFT") of the two measured signals. For sinusoidal signals there is only one non-zero spectral line in the basic DFT spectrum interval if integer number of periods is sampled.

The FTD spectra of the discrete-time signals $v_1(nT)$ and $v_2(nT)$ (both of the length NT (s) are

$$\mathbf{V}_i(e^{j\omega T}) = \sum_{n=-\infty}^{\infty} v_i(nT) e^{-j\omega_{sig} nT} = \sum_{n=0}^{N-1} v_i(nT) e^{-j\omega_{sig} nT} \quad i = 1 \text{ or } 2, \quad (15)$$

where N is the number of processed samples, ω_{sig} is signal circular frequency, and T is sampling interval. The two measured signals $v_1(nT)$ and $v_2(nT)$ are zero for $0 > n \geq N$. Since there is

$$e^{-j\omega_{sig} nT} = \cos(\omega_{sig} nT) - j \sin(\omega_{sig} nT), \quad (16)$$

(14) can be re-written as

$$\mathbf{V}_i(e^{-j\omega T}) = \sum_{n=0}^{N-1} v_i(nT) (\cos(\omega nT) - j \sin(\omega nT)). \quad (17)$$

The DFT spectrum is formed by samples of the FTD spectrum at circular frequencies $\omega_k = k \times (\omega_s/N)$ and it can therefore be written as

$$\mathbf{V}_i\left(\frac{k\omega_s}{N}\right) = \sum_{n=0}^{N-1} v_i(nT) \left(\cos\left(\frac{k\omega_s}{N} nT\right) - j \sin\left(\frac{k\omega_s}{N} nT\right) \right). \quad (18)$$

The phase of the two sinusoidal signals $v_i(nT)$ φ_i , $i = 1, 2$, can be found as

$$\varphi_i = \arctg \frac{\text{Im}(\mathbf{V}_i(e^{-j\omega_k T}))}{\text{Re}(\mathbf{V}_i(e^{-j\omega_k T}))} = \frac{\sum_{n=0}^{N-1} v_i(nT) \sin\left(\frac{2\pi}{N} nk\right)}{\sum_{n=0}^{N-1} v_i(nT) \cos\left(\frac{2\pi}{N} nk\right)} \quad i = 1 \text{ or } 2. \quad (19)$$

Circular frequencies for which the DFT spectrum is calculated are $k(\omega_s/N)$ (they form a so-called „DFT grid”). That is why argument of reference signals in (12) and (13) (i.e. $\omega_{sig}nT$) is identical with arguments of sine and cosine function in (19) i.e. there is $\omega_{sig}nT = (2\pi/N)nk$. Processing of input samples by VVV and DFT method is therefore from mathematical point of view the same, and that is why the bias and standard deviations of those two methods give the same results. If not integer number of signal periods is sampled, there is identical nonzero bias of these algorithms. In the DFT spectrum the well known „leakage” effect takes place in this case and the spectrum of sinusoidal signal is composed of many nonzero spectral lines.

The computing time of VVV and DFT algorithm might not be exactly the same, since e.g. DFT is in practice most frequently calculated using FFT algorithms and not the DFT definition formula. The DFT computing time is therefore usually shorter than the VVV computing time.

Owing to the spectral leakage in case of non-coherent sampling, signals are multiplied by windows and the so - called interpolated DFT is used [8]-[10]. Phase difference bias is lower by non-coherent sampling if interpolated DFT (denoted “IDFT” algorithm here) is used. By using interpolated DFT, the exact frequency of signal is found between positions of the two largest spectral components of amplitude frequency spectrum. The known spectrum of the used window is used for finding value of the frequency displacement, i.e. the decimal value of frequency that has to be added to the frequency of the first of two largest components of the amplitude frequency spectrum to get the signal frequency. Simplified formulae derived for given window used are applied for frequency finding. After having found the signal frequency, signal RMS value and phase can be found. The phase difference is found as difference of phases of the two measured signals. Hann window is used most frequently. We have used it in the simulations and measurements presented in this paper as well, even if our program allows using cosine windows of the order up to 4. The DFT is also in interpolated algorithms calculated using FFT algorithms. Signal frequency, amplitude and phase can be found using this method.

Two other modifications of the DFT interpolated in frequency domain are described in [9] and [10]. Interpolation in frequency domain without signal windowing (i.e. using rectangular windows) is used in [9] In the recent paper of the same author [10] uses a more sophisticated interpolation formulae (up to three points interpolation), and Hann window can also be used. We have included the algorithm from [10] in our program, based on two-point interpolation and using Hann window. Comparison of measurement bias, type A standard measurement uncertainty and computing time of this method (denoted as “IDFTA”, for Interpolated DFT suggested by Prof. Agrez) with our interpolated DFT (usable for applying Rife-Vincent windows of the first class and interpolation formula from [8]) is presented in part IV devoted to simulations.

2.4. Methods based on sine-wave-fits (SWFM, SWF3p, SWFF4p, SWFR)

A powerful tool for phase difference measurement are the sine-wave-fit techniques, based on least-square error (LSE) between (the samples of) the measured signal and (samples of) an ideal sinusoid. This sinusoid is characterized by 3 (magnitude, frequency and phase) or 4 (nonzero DC component added) parameters found for getting minimum LSE. If applied on both the measured signals, phase difference is obtained as the difference of phases of the both measured signals. These methods can provide apart from phase also values of signal amplitude, frequency and in case of 4-parameter methods also the DC component, and are described in [5] (method designed especially for measurement of phase difference -“SWFM”) or in the standard [12] (realization of this method named here “SWFF3p” and “SWFF4p” use MATLAB function *fminsearch* for finding minimums of functions of several variables with 3 or 4 parameters). Recently the 7-parameters sine-wave-fit modification supposing the same

frequency of both signals and finding all 7 parameters of the two sinusoids with identical frequency was published [11] (method denoted here as “SWFR”). All 7 parameters are being found in a common iteration process, and this method is compared in [11] with 3 and/or 4 parameter sine-wave-fit procedures applied separately to each measured signal.

The SWFM and SWFR algorithms were found by us to be the best ones both from the point of accuracy and computation time (if implemented in MATLAB). A brief information about their mathematical background (presented in more detailed way in [5] and [11]) is given here.

The *sine-wave-fit algorithm proposed by R. Micheletti* [5] (denoted here as SWFM algorithm) is the least-square-error based algorithm, allowing finding parameters (magnitude and phase) of a sinusoidal waveform placed on a sequence of signal samples. The algorithm is applied on sequences of samples of two sinusoidal signals $v_1(t)$ and $v_2(t)$ (mixed in practice with additive noise). The signals are sampled at the same sampling frequency f_s and M samples of each signals is taken. The same frequency and zero DC components are supposed by both the signals the phase difference of which is to be found. The procedure described in [5] is as follows.

The two processed signals are given in (1) and (2) and can be re-written as

$$v_1(t) = V_1 \cos \varphi_1 \cdot \sin \omega \cdot t + V_1 \sin \varphi_1 \cdot \cos \omega \cdot t = C_0 \sin \omega \cdot t + C_1 \cos \omega \cdot t, \quad (20)$$

$$v_2(t) = V_2 \cos \varphi_2 \cdot \sin \omega \cdot t + V_2 \sin \varphi_2 \cdot \cos \omega \cdot t = D_0 \sin \omega \cdot t + D_1 \cos \omega \cdot t, \quad (21)$$

where

$$C_0 = V_1 \cos \varphi_1 \quad D_0 = V_2 \cos \varphi_2, \quad (22)$$

$$C_1 = V_1 \sin \varphi_1 \quad D_1 = V_2 \sin \varphi_2 \quad (23)$$

and

$$V_1 = \sqrt{C_0^2 + C_1^2}, \quad \varphi_1 = \tan^{-1} \left[\frac{C_0}{C_1} \right] + [1 - \text{sgn}(C_0)] \frac{\pi}{2}, \quad (24)$$

$$V_2 = \sqrt{D_0^2 + D_1^2}, \quad \varphi_2 = \tan^{-1} \left[\frac{D_0}{D_1} \right] + [1 - \text{sgn}(D_0)] \frac{\pi}{2}. \quad (25)$$

Using the LSE algorithm, parameters C_j, D_j ($j=1$ or 2) can be found using the equations

$$\frac{\partial}{\partial C_j} \left\{ \sum_{r=0}^{M-1} \left[\sum_{s=0}^1 C_s \Phi_s(t_r) - v_1(t_r) \right]^2 \right\} = 0, \quad (26)$$

$$\frac{\partial}{\partial D_j} \left\{ \sum_{r=0}^{M-1} \left[\sum_{s=0}^1 D_s \Phi_s(t_r) - v_2(t_r) \right]^2 \right\} = 0, \quad (27)$$

where $\Phi_0(t) = \sin \omega t$ a $\Phi_1(t) = \cos \omega t$, and

$$\sum_{r=0}^{M-1} \left[\Phi_i(t_r) \sum_{s=0}^1 C_s \Phi_s(t_r) \right] = \sum_{r=0}^{M-1} \Phi_i(t_r) v_1(t_r), \quad (28)$$

$$\sum_{r=0}^{M-1} \left[\Phi_i(t_r) \sum_{s=0}^1 D_s \Phi_s(t_r) \right] = \sum_{r=0}^{M-1} \Phi_i(t_r) v_2(t_r), \quad (29)$$

where $v_1(t_r)$ and $v_2(t_r)$ are discrete-time samples of the two sinusoidal signals, and $i = 1$ or 2 . These equations can be written in matrix form as

$$\mathbf{A}^T \mathbf{A} \mathbf{C} = \mathbf{A}^T \mathbf{b}, \quad (30)$$

$$\mathbf{A}^T \mathbf{A} \mathbf{D} = \mathbf{A}^T \mathbf{g}, \quad (31)$$

where

$$\mathbf{A} = \begin{bmatrix} \sin \omega t_0 & \cos \omega t_0 \\ \sin \omega t_1 & \cos \omega t_1 \\ \dots & \dots \\ \sin \omega t_{M-1} & \cos \omega t_{M-1} \end{bmatrix}, \quad \mathbf{C} = \begin{bmatrix} C_0 \\ C_1 \end{bmatrix}, \quad \mathbf{b} = \begin{bmatrix} v_1(t_0) \\ v_1(t_1) \\ \dots \\ v_1(t_{M-1}) \end{bmatrix}, \quad \mathbf{D} = \begin{bmatrix} D_0 \\ D_1 \end{bmatrix}, \quad \mathbf{g} = \begin{bmatrix} v_2(t_0) \\ v_2(t_1) \\ \dots \\ v_2(t_{M-1}) \end{bmatrix}$$

and

$$\mathbf{A}^T \mathbf{A} = \begin{bmatrix} \sum_{r=0}^{M-1} \sin^2 \omega t_r & \frac{1}{2} \sum_{r=0}^{M-1} \sin 2\omega t_r \\ \frac{1}{2} \sum_{r=0}^{M-1} \sin 2\omega t_r & \sum_{r=0}^{M-1} \cos^2 \omega t_r \end{bmatrix}. \quad (32)$$

Matrix $\mathbf{A}^T \mathbf{A}$ can be calculated in advance and stored in a table, since it depends only on sampling frequency and number of samples per period.

The phase difference of the two signals is found as

$$\varphi = \varphi_1 - \varphi_2. \quad (33)$$

The 7-parameters sine-wave-fit method proposed by P.M.Ramos, F. Da Silva and A. Cruz Serra [11] (denoted here as SWFR algorithm) enables the user to find magnitudes, phases and DC components of two digitized sinusoidal signals of the same frequency, using again the LSE minimization algorithm. This method is an extension to the sine-wave-fit methods described in standard [12].

Here again the both measured signals are sampled at the sampling frequency f_s and M samples is taken from each of the signals. Values of these samples are denoted $y_{1,1}, y_{1,2} \dots y_{1,M}$ for the first signal and $y_{2,1}, y_{2,2} \dots y_{2,M}$ for the second signal. Time instants in which the samples are taken are denoted $t_{k,n}$, where $k = 1, 2$ denotes the signal, and $n = 1, 2, \dots, M$ is index of the sample. Contrary to the expressions for the processed signals (1) and (2), non-zero DC components of the signals are allowed here.

The matrices used in the 7-parameter method are

$$\mathbf{D}_{k,i} = \begin{bmatrix} w(f_{k,i}, t_{k,1}) & g(f_{k,i}, t_{k,1}) & 1 & h(A_{k,i-1}, B_{k,i-1}, f_{k,i}, t_{k,1}) \\ w(f_{k,i}, t_{k,2}) & g(f_{k,i}, t_{k,2}) & 1 & h(A_{k,i-1}, B_{k,i-1}, f_{k,i}, t_{k,2}) \\ \vdots & \vdots & \vdots & \vdots \\ w(f_{k,i}, t_{k,M}) & g(f_{k,i}, t_{k,M}) & 1 & h(A_{k,i-1}, B_{k,i-1}, f_{k,i}, t_{k,M}) \end{bmatrix}, \quad (34)$$

where

$$w(f, t) = \cos(2\pi f t),$$

$$g(f, t) = \sin(2\pi ft), \quad (35)$$

$$h(A, B, f, t) = -At \sin(2\pi ft) + Bt \cos(2\pi ft).$$

The matrix used in iteration procedure in this method has $2M$ rows and 7 columns:

$$\mathbf{D}_i = \begin{bmatrix} Q_{1,i} & R_{1,i} & 0 \\ 0 & R_{2,i} & Q_{2,i} \end{bmatrix}, \quad (36)$$

where

$$\mathbf{Q}_{k,i} = \begin{bmatrix} w(f_i, k_{k,1}) & g(f_i, k_{k,1}) & 1 \\ w(f_i, k_{k,2}) & g(f_i, k_{k,2}) & 1 \\ \vdots & \vdots & \vdots \\ w(f_i, k_{k,M}) & g(f_i, k_{k,M}) & 1 \end{bmatrix} \quad (37)$$

and

$$\mathbf{R}_{k,i} = \begin{bmatrix} h(A_{k,i-1}, B_{k,i-1}, f_i, t_{k,1}) \\ h(A_{k,i-1}, B_{k,i-1}, f_i, t_{k,2}) \\ \vdots \\ h(A_{k,i-1}, B_{k,i-1}, f_i, t_M) \end{bmatrix}. \quad (38)$$

The resulting vector is

$$x = [A_1 \ B_1 \ C_1 \ f \ A_2 \ B_2 \ C_2]^T, \quad (39)$$

where A and B define amplitude and phase of signals 1 and 2, C are DC components of these signals and f is signal frequency, is found from the matrix equation

$$x = [D^T D]^{-1} [D^T y], \quad (40)$$

where D is matrix of the last iteration and D^T is transposed matrix of the last iteration.

Iteration finishing criterion is given by the chosen relative deviation of the frequency found in iteration process from the known signal frequency. In our algorithm implementation it was $\delta f_i < 10^{-7}$.

Besides the two above-described algorithms, we used also the MATLAB function *fminsearch* for finding the phase difference of the two measured sinusoidal signals represented by two sequences of signal samples (denoted in this paper as SWFF3p and SWFF4p). The function *fminsearch* is designed for finding minimums of functions of several variables. It can be used with 3 or 4 parameters (modifications „3p” and „4p” of the SWFF) if used in sine-wave-fit applications. The „3p” version is used for input signals with zero DC component. The *fminsearch* function is much more generally usable than the two above mentioned single-task sine-wave-fit LSE algorithms. Its mathematical background is much more complicated and is only briefly mentioned in MATLAB help. As was found by our experiments, using this function needs much higher computation time, and for the approximately the same accuracy also much higher number of processed samples than the SWFM and SWFR algorithms.

3. GRAPHICAL USER INTERFACE USED

Since many simulations and measurements had to be performed for comparison of the sensitivity of the above mentioned methods to different influences, a graphical user interface was designed in MATLAB allowing easy modification of parameters of signals, range and resolution of the ADC (in simulations), number of signal samples processed and sampling frequency (desired non-integer number of periods can be selected), noising the signals by additive noise for selected SNR and distorting signals with higher-order harmonic components (up to the order 50, with random phases and magnitudes related to the fundamental harmonic components according to compatibility levels given by the international LF EMC standards (e.g. [13])). This GUI allows selection of methods to be applied for given simulation or measurement and selection of quantity that should be used as independent variable for presentation of results. The output graphs can be easily modified in MATLAB, and 7 different output figures are at the user disposal after finishing the measurement or simulation.

4. RESULTS OF SIMULATIONS

Selected results allowing comparison of the investigated methods are presented here. The presented results of simulations and measurement allow comparison of algorithms from the point of view of their sensitivity to sampling of non-integer number of signal periods (“non-coherent sampling”), sensitivity to additive noise, to signal *THD* (total harmonic distortion), and to non-zero DC component. Figures are shown for 12-bit signal quantization, both signals magnitudes 5 V, frequency 50 Hz and phase difference 50 deg, ADC range is 5 V. Number of repeated simulations was 1000, sampling frequency 6400 Hz (128 Sa/per). Fig. 2 to Fig. 7 are plotted for $SNR = 70$ dB, $THD = 0.16$ % (corresponding to the *THD* of the signals generated by the generator used in measurements – see section V), 128 Sa/per (sampling frequency 6400 Hz) and for 2 to 12 periods sampled. The simulation results shown in Fig. 2 to Fig. 7 are grouped according to Section II into three groups (method VVV was added to DFT, since their results are identical; the reason of this was shown above).

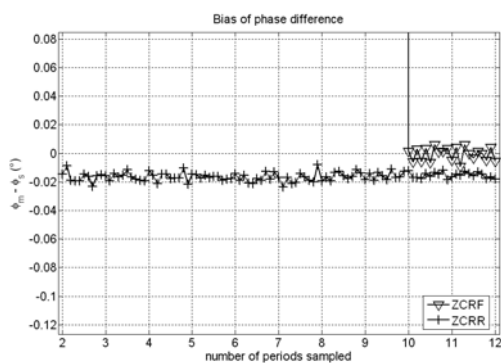


Fig. 2. Bias of ZCRF and ZCRR methods, SNR=70 dB.

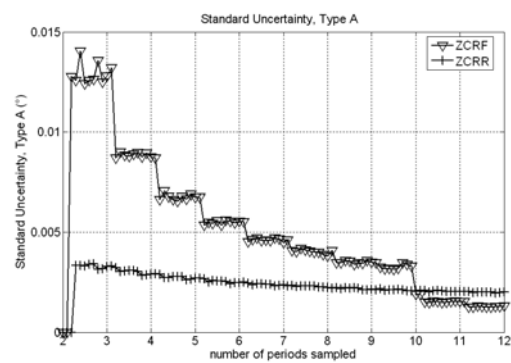


Fig. 3. Standard deviation of ZCRF and ZCRR methods, SNR=70 dB.

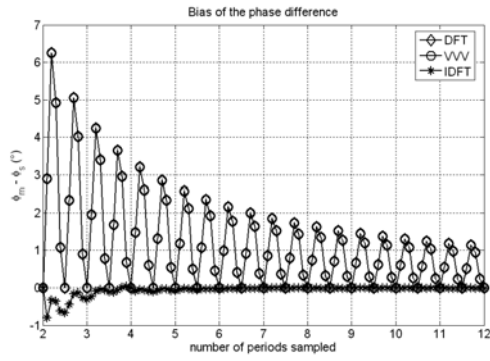


Fig. 4. Bias of DFT, VVV and IDFT methods, SNR=70 dB.

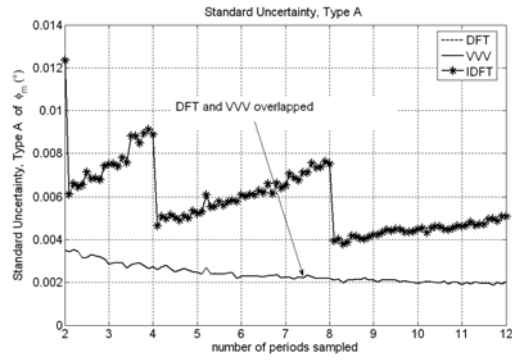


Fig. 5. Standard deviation of DFT, VVV and IDFT methods, SNR=70 dB.

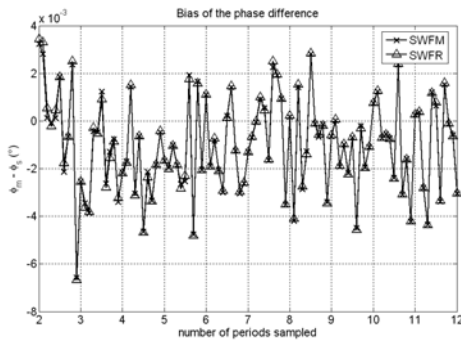


Fig. 6. Bias of SWFR and SWFM methods, SNR=70 dB.

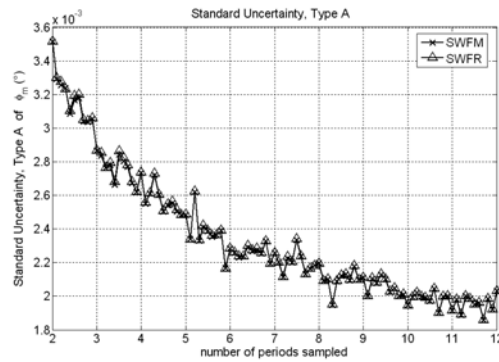


Fig. 7. Standard deviation of SWFR and SWFM methods, SNR=70 dB.

The ZCRF method results for the first 10 periods sampled were ignored in processing to exclude the transient component of the filter output (see Fig. 2 and Fig. 3).

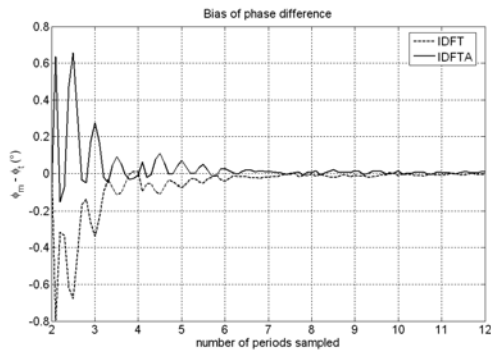


Fig. 8. Bias of IDFT and IDFTA [10] methods.

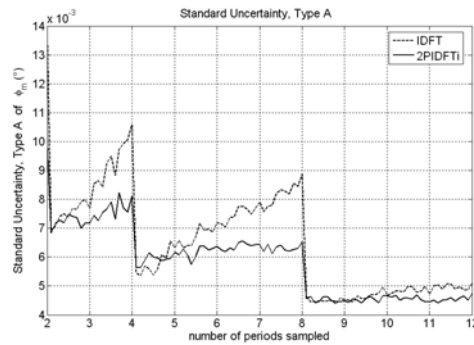


Fig. 9. Standard deviation of IDFT and IDFTA [10] methods.

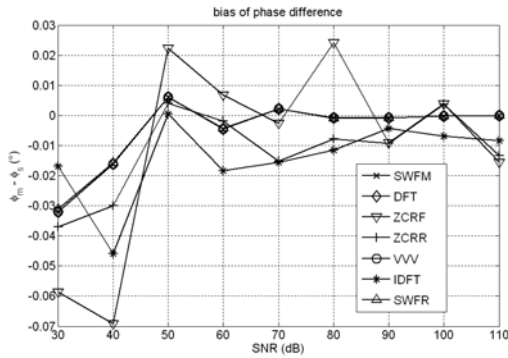


Fig. 10. Bias of investigated methods as a function of SNR (10.5 signal periods sampled, THD=5%).

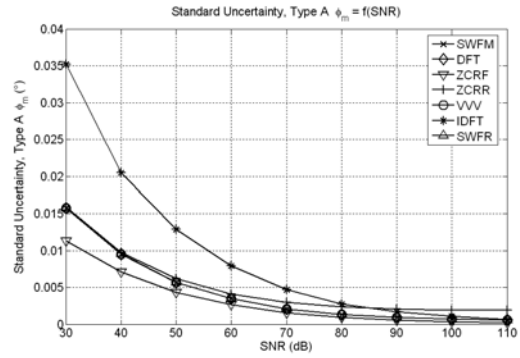


Fig. 11. Standard deviation as a function of SNR (10.5 signal periods sampled, THD=5%).

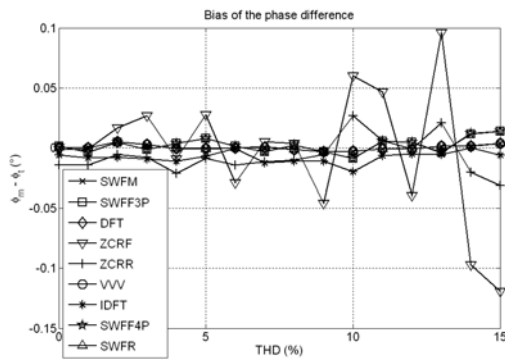


Fig. 12. Bias investigated methods as a function of THD (10.5 signal periods sampled).

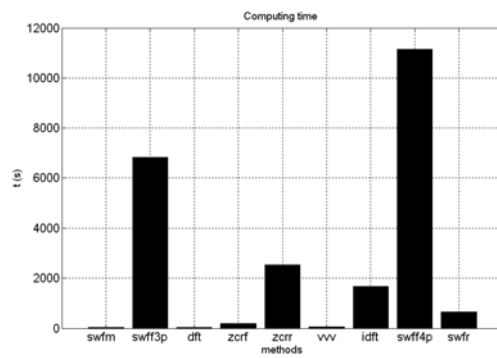


Fig. 13. Computing time of the investigated methods.

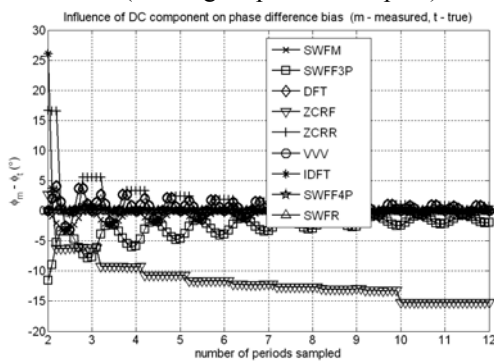


Fig. 14. Influence of DC component on bias (one signal has 1 V DC component), all methods.

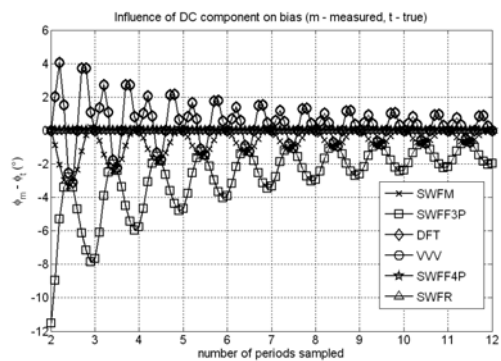


Fig. 15. Influence of DC component (one signal has 1 V DC component), without ZCRF, ZCRR and IDFT methods.

5. RESULTS OF MEASUREMENTS

Measurements were performed on two output signals of the generator HP 3245A. The both measured signals were sine signals with frequency 50 Hz, amplitudes 5 V. Their phase difference was set to 50 deg, number of measurements was 100. Peak-to-peak voltage was 5 V, the THD of the generated sinusoidal signal is $\text{THD} < 0.16\%$. (Some measurements were performed using sinusoidal signals generated by two function/arbitrary generators Agilent 33220A, equipped with external frequency reference and phase-locked loop options, allowing phase adjustment via computer interface. *THD* of generators is 0.04%. These generators were found to generate less stable than the HP 3245A generator, and therefore measurement results

gained from HP 3245A are presented here.)

The measurement were performed for the SNR = 70 dB, so that they can be compared with the simulation results (Fig. 2 to Fig. 7). The additive noise was generated by software. The two measured signals were sampled by a 12-bit multifunction DAQ PC plug-in board National Instruments NI 6023E. The sampling rate 128 Sa/period (sampling frequency $f_s = 6400$ Hz per channel was used). The plug-in board setting and signal sampling was controlled by means of Data Acquisition Toolbox of MATLAB.

As can be seen from Fig. 22 and Fig. 23, bias of SWFF methods is larger than that of the other sine-wave fit methods (SWFM and SWFR) for given sampling frequency. The computation time of SWFF methods is much higher than the computation time of the rest of the investigated methods. For the used sampling with 128 Sa/per their results had bias about 1.4 deg (see Fig. 22), which corresponds very good with the dependence of their results on sampling frequency (Fig. 23). Other methods with low bias are included in Fig. 23 to show what is the approximate value of the “true” phase difference.

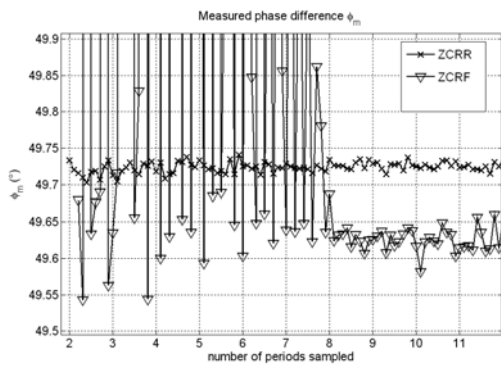


Fig. 16. Phase difference by ZCRR and ZCRF methods.

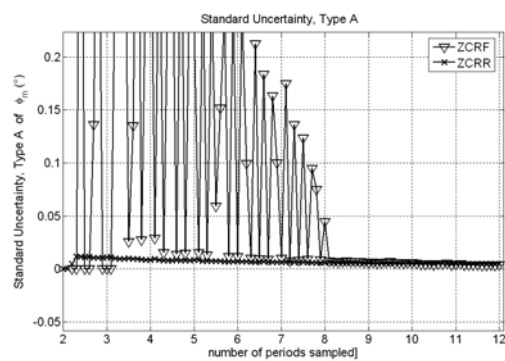


Fig. 17. Standard deviation of ZCRR and ZCRF methods.

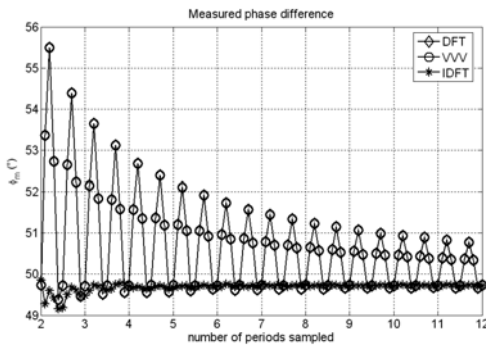


Fig. 18. Phase measured by DFT, VVV and IDFT methods.

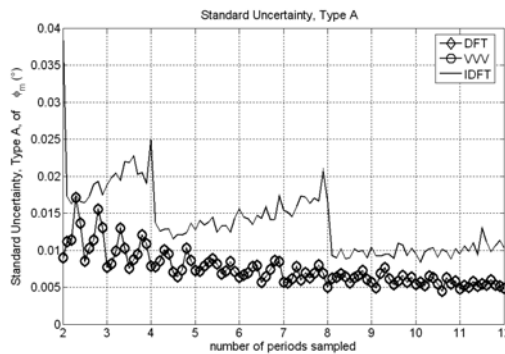


Fig. 19. Standard deviation of measurements by DFT, VVV and IDFT methods.

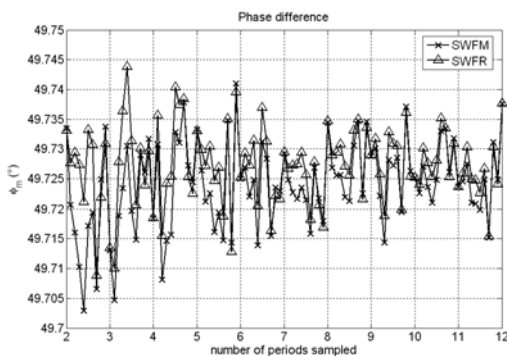


Fig. 20. Phase measured by SWFM and SWFR

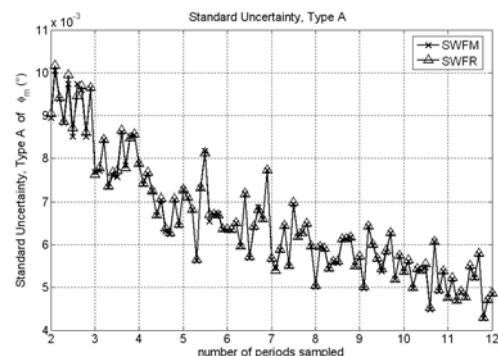


Fig. 21. Standard deviation of measurements by

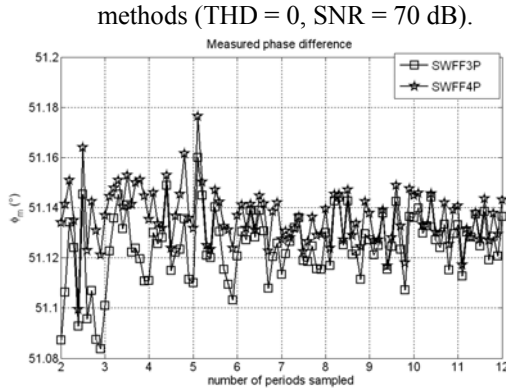


Fig. 22. Phase difference by SWFF3p and SWFF4p methods, measurement (THD = 0, SNR = 70 dB).

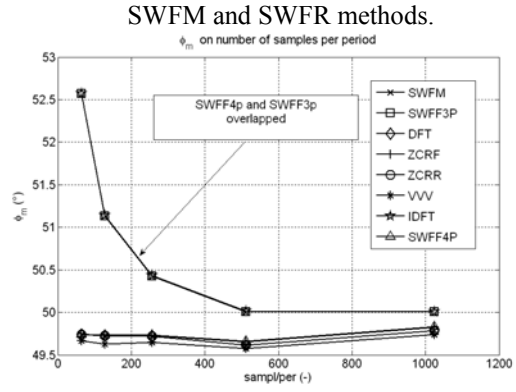


Fig. 23. Influence of number of samples on SWFF bias (phase difference is 50 deg, measurement).

The figures 19 to 21 present the same methods as Figs. 2 to 7 for simulations, but since the true phase shift is not known in general by measurements (and the MATLAB program for measurement is respecting this fact), measured values of phase difference are presented here instead of the bias of the phase difference shown by simulations.

6. CONCLUSIONS

As can be seen from the figures above, methods DFT and VVV are not suitable for non-coherent sampling (sampling not integer number of periods). Sensitivity of the DFT method to sampling non-integer number of periods (i.e. to leakage effect) is substantially reduced by signal windowing and interpolation (see IDFT and IDFTA method results). Bias caused by leakage is decreasing with number of periods sampled. The results of IDFT method shown in Fig. 4, Fig. 5, Fig. 18 and Fig. 19, Fig. 8 and Fig. 9 (together with IDFTA) are plotted for Hann window used. If higher-order windows were used for signal windowing in IDFT method, so many signal periods have to be sampled that the main lobes of window spectrum placed at frequencies of neighbouring signal harmonic components do not overlap.

Computing time of IDFTA algorithm was found to be approximately five times shorter than computing time of IDFT algorithm, magnitude of bias of the IDFT and IDFTA is practically the same

Methods DFT and VVV give the same results since mathematical processing of signal samples is in fact the same for these methods, as was derived in parts II B and II C. That is why the graphs of phase difference and standard deviations (type A standard uncertainties) of these methods overlap in all figures. The computing times of these methods may not be identical, as was explained in part II C, and since FFT algorithm is usually used in DFT calculation, DFT computing time is in most cases shorter than that of VVV (see e.g. Fig. 17).

Method of ZCRF used with LP FIR filter to suppress the additive noise before zero-crossing detections is usable in our implementation only for more than 10 periods sampled (see Fig. 2 and Fig. 3) to exclude the filter output transient. A slight modification of this algorithm allows subtracting mean of the filter output signal

The presented results of simulations and measurements show that from the point of view of *measurement bias* the sequence of the investigated methods is for non-coherent sampling for the same sampling frequency and number of samples ordered from the best one to the worst one following: SWFR, SWFM, ZCRR, IDFT and IDFTA (depending on number of periods sampled and window order used in signal windowing), ZCRF, SWFF3p and SWFF4p.

As can be seen from the figures above, from the point of view of *measurement uncertainty*

(type A) the sequence of the investigated methods is for non-coherent sampling is similar to the sequence ordered by phase bias.

From the point of view of *computation time* (programmed in MATLAB) the sequence of the investigated methods is approximately (from the best one to the worst one, computation times given in relative scale): SWFM (1), DFT (1.1), VVV (1.6), IDFTA(7), SWFR (11), ZCRF (16), IDFT (36), ZCRR (59), SWFF3p (350), SWFF4p (610). The slowest – SWFF - methods require moreover larger numbers of samples to reach bias comparable to other methods (see Fig. 14 and Fig. 15).

Sensitivity of the investigated methods to the *additive noise* can be from Fig. 10 and Fig. 11. Methods ZCRF, ZCRR and IDFT are most sensitive to additive noise (to SNR), methods SWFR, SWFM and DFT are the least sensitive to SNR.

Sensitivity of investigated methods oh harmonic distortion of measured signals (on THD) can be seen fro Fig.12: The most sensitive methods are ZCRF, ZCRR, IDFT, and both SWFF methods, the best methods here are SWFR, SWFM. DFT and VVV.

Sensitivity of methods to nonzero DC component was tested by adding a DC component 1 V to one of the measured signals. Influence of this component on the pphase difference bias can be seen from Fi. 14 and Fig. 15: The most sensitive are methods ZCRF, ZCRR, SWFF3p and IDFT (bias of DFT and VVV methods in this figure is caused by nen-coherent sampling, not by a DC component), methods with lowest sensitivity to DC components are (as can be expected because of their principle) the SWFR and SWFF4p.

It follows from the information given above that the sine-wave-fit methods SWFR [11] and SWFM [5] are the best ones from the compared methods from the point of view of both measurement bias and type A uncertainty, both for sampling integer and non-integer number of periods. The SWFM method is at the same time the fastest one (by programming the methods in MATLAB), but contrary to SWFR it is sensitive to the signal DC component (see Fig. 14 and Fig. 15).

ACKNOWLEDGEMENT

This research was supported by the research program No. MSM6840770015 "Research of Methods and Systems for Measurement of Physical Quantities and Measured Data Processing" of the CTU in Prague sponsored by the Ministry of Education, Youth and Sports of the Czech Republic.

REFERENCES

1. Krumpholc M., Sedlacek M: *Measurement of phase difference using DSP algorithms by non-coherent sampling*, Proc. of the 14th International Symposium on New Technologies in Measurement and Instrumentation, IMEKO TC-4, vol. I, Gdynia, Poland, September 2005, pp. 229-234.
2. Ibrahim K.M., Abdul-Karim M.A.H.: *A Novel Digital Phase Meter*, IEEE Trans. Instrum. Meas., vol. IM-36, no. 3, October 1989, pp. 711-715.
3. Wagdy M.F, Lucas, M. S. P.: *Errors in Sampled Data Phase Measurement*, IEEE Trans. Instrum. Meas., vol. IM-34, no. 4, December 1985, pp. 507-509.
4. Mahmud S. M: *High Precision Phase Measurement Using Adaptive Sampling*, IEEE Trans. Instrum. Meas., vol. 38, no. 5, October 1989, pp. 954-960
5. Micheletti, R.: *Phase Angle Measurement Between Two Sinusoidal Signals*, IEEE Trans. Instrum. Meas., vol. 40, no. 1, February 1991 pp. 6-9.
6. Sedlacek M.: *Digital measurement of phase difference of LF signals - a comparison of DSP algorithms*, Proc. of XVII IMEKO World Congress, Dubrovnik, June 2003, pp. 639-644.
7. Schoukens J., Pintelon R., Van hamme H: *The interpolated Fast Fourier Transform: A Comparative Study*, IEEE Trans. Instrum. Meas., vol. 41, no. 2, April 1992, pp. 226-232.
8. Andria G., Savino, M., Trotta A: *Windows and Interpolation Algorithms to Improve Electrical Measurement Accuracy*, IEEE Trans. Instrum. Meas., vol. 38, no. 4, August 1989, pp. 856-863.
9. Agrez D.: *Interpolation in the frequency domain to improve phase measurement*, Proc. of XVII IMEKO World Congress, Dubrovnik, June 2003, pp. 446-450.

10. Agrez D.: *Improving Phase Estimation With Leakage Minimization*, IEEE Trans. Instrum. Meas., vol. 54, no. 4, pp. 1347-1353, August 2005, pp. 1347-1353.
11. Ramos P. M., Da Silva F., Cruz Serra V: *Improving sine-fitting algorithms for amplitude and phase measurements phase measurements*, Proc. of XVII IMEKO World Congress, Dubrovnik, June 2003, pp. 614-619.
12. IEEE Std. 1241-2000 *Standard for Analog to Digital Converters*, New York, 2001.
13. IEC 61000-2-2, *Electromagnetic Compatibility, Part.2 – Environment, Section 2: Compatibility levels for LF conducted disturbances and signaling in public low-voltage power supply systems*, IEC, Switzerland, 1990.
14. Enden A., W. M., Verhoeck, N. A. M: *Discrete-Time Signal Processing*, Prentice Hall, 1989.

CYFROWY POMIAR PRZESUNIĘCIA FAZOWEGO – STUDIUM PORÓWNAWCZE ALGORYTMÓW CPS

Streszczenie

W artykule porównano 10 metod pomiaru przesunięcia fazowego pod względem ich wrażliwości na niecałkowitą liczbę próbek w okresie sygnału. Rozpatrywane metody zostały podzielone na 4 grupy – zmodyfikowane metody oparte na detekcji przejścia przez zero, pomiary bazujące na DFT, metody wirtualnego woltomierza wektorowego i zmodyfikowane algorytmy dopasowania przebiegów sinusoidalnych. Przedstawiono wyniki symulacji i pomiarów.